ACS Biomaterials SCIENCE & ENGINEERING

pubs.acs.org/journal/abseba

Article

Regulation of Chondrocyte Differentiation by Changing Intercellular Distances Using Type II Collagen Microfibers

Jinyu Li, Naoko Sasaki, Keiji Itaka, Margo Terpstra, Riccardo Levato, and Michiya Matsusaki*

Cite This: *ACS Biomater. Sci. Eng.* 2020, 6, 5711−5719

Read Online

ACCESS | Metrics & More | Article Recommendations | Supporting Information

ABSTRACT: Osteoarthritis is a common degenerative disease that mainly occurs in older age groups, and the search for an effective cure remains a major global challenge. The technology of constructing 3D in vitro cartilage tissue with zonal differentiated structures for use as alternative implants for treating osteoarthritis has attracted researchers' attention. For this challenge, it is important for understanding the relationship between chondrocyte differentiation and the amount of extracellular matrix by modulating intercellular distance. This study investigates the interplay between chondrocyte differentiation and intercellular distance. Type II collagen microfibers (CMF II) were used as a distance regulator by varying their amounts. The results indicated that the secretion of cartilage-specific glycosaminoglycan after 2 weeks of differentiation from the chondrogenic cells, ATDC5, was decreased with an increased intercellular distance. Also, the shortest intercellular distance, being ATDC5 cells without CMF II, presented an upregulated gene expression profile of cartilage markers. The groups with CMF II-mediated intracellular distances, however, did not show the upregulation. The elastic modulus of the 3D samples increased depending on the amount of CMF II, relating to the differentiation preventing property of the CMF II. These findings suggest the promising potential of this approach for the modulation of chondrocyte differentiation.

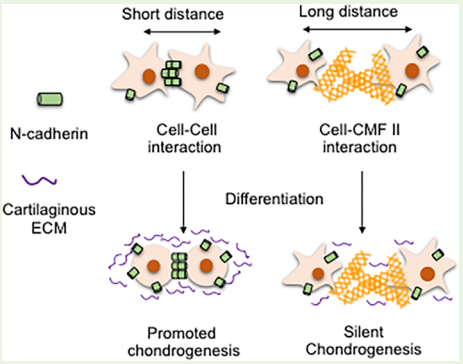

KEYWORDS: *collagen microfiber, intercellular distance, chondrocyte differentiation, tissue engineering, cartilage*

1. INTRODUCTION

Osteoarthritis is a severe joint disease that is mostly induced by mechanical injuries or the effects of aging. According to the Global Burden of Disease, Injuries, and Risk Factors Study 2015, 237 million, or around 3.3% of people worldwide suffer from this disease.[1] Unfortunately, the regeneration of newly engineered cartilage tissue is still a major challenge. The main reason for this is that cartilage tissue is an avascular, alymphatic, and aneural tissue with a poor recovery capacity also caused by insufficient delivery of therapeutic biological signals. Current therapeutical approaches such as invasive joint replacement prosthesis have limited lifespan and cell therapy based on autologous cartilage implantation (ACI) also offers only a temporary solution, mainly resulting in the formation of a repair tissue with limited mechanical properties. This procedure is also rendered more challenging by the fact that chondrocytes expanded in 2D are prone to dedifferentiate.[2] The construction of 3D cartilage tissue in vitro might therefore be a promising approach to address these issues.

Notably, cartilage tissues are characterized by a zonal organization that consists of a superficial, middle, and deep zone. Recent reports have revealed that the chondrocytes located in different zones behave diversely. Generally, chondrocytes located in the deep zone have a more mature phenotype and produce higher amounts of proteoglycans.[3,4] Consequently, the deep zone display the highest mechanical strength.[5] To create functional 3D cartilage tissues for wide applications, the construction of zonal cartilage tissues differentiation gradient is vital. In earlier studies, a scaffold-free method has been shown to be a straightforward way of achieving the desired differentiation degree by activating the condensation potential of mesenchymal stem cells (MSCs).[6] However, although scaffold-free cartilage tissues have recently become one of the standard methods, they lacks zonal organization.[7] As an alternative to scaffold-free methods, scaffold-based technological approaches can be chosen, using biocompatible functional materials, such as gelatin,[8] alginate,[9] and silk fibroin.[10] Using these materials still does not lead to zonally organized tissues structure. One approach to achieve an engineered tissue with distinct zones can be to sort and reseed cells with a distinct chondrogenic behavior in a gradient-like fashion. Significant challenges have been reported to isolate cell subpopulations and to reconstruct zonally organized tissues. For instance, chondrocytes originating from different zones were sorted based on size diversity,[11] but harvested cells

Received: March 26, 2020
Accepted: September 1, 2020
Published: September 1, 2020

https://dx.doi.org/10.1021/acsbiomaterials.0c00427
ACS Biomater. Sci. Eng. 2020, 6, 5711−5719

are not so pure due to the slight size change of chondrocytes derived from middle and deep zones. Previous work showed the potential of encapsulating articular cartilage-resident chondroprogenitor cells (ACPCs) and bone marrow-derived MSCs in different layers of one constructs to mimic the native zone-specific distribution of cartilage markers.[12] Besides using different sorted cell populations, chondrocyte-laden hydrogels with a gradient of mechanical stiffness was generated to conserve the zonal differentiation structure through the stimulation of mechanosensing pathways.[13] The production of type II collagen showed an opposite trend to native cartilage, the softer zone indicated a higher amount of the type II collagen.

To achieve the construction of zonal cartilage tissues, fundamental knowledge on the correlation between chondrocyte differentiation and ECM concentration, especially type II collagen is essential. Collagen accounts for 10−30 wt % of the articular cartilage matrix and its major component is type II collagen, occupying 90−95 wt %.[14] More importantly, type II collagen has an effect on inhibiting terminal differentiation of hypertrophy by activating integrin β1 to interfere with the bone morphogenetic protein-SMAD1 pathway.[15] However, there is still no report regarding the effect of the type II collagen amount in the intercellular and pericellular territory on chondrocyte differentiation. Besides, previous works have illustrated the critical role of cell−cell interaction in stimulating chondrogenesis and, as an effect, in boosting type II collagen secretion.[16] The cell adhesion molecule N-cadherin and gap junction proteins connexin 43 are considered to be a main access for intercellular communication through a mechanosensitive pathway, which have proven influence on promoting the chondrogenesis, especially in the early mesenchymal condensation stage during limb development.[17−19] On the basis of these findings, it is hypothesized that shortening the intercellular distance would facilitate the chondrogenesis. In contrast, increasing the intercellular distance by increasing the type II collagen amount may interfere with adhesion molecules conjugation that prevents cell−cell interaction (Figure 1).

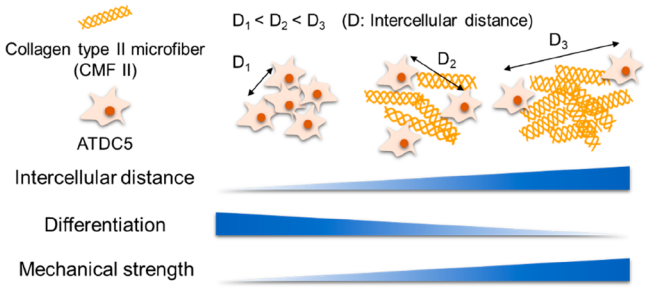

Figure 1. Controlling the cartilage tissues' behavior by adjusting the intercellular distances using CMF II.

We recently reported a novel technique, sedimentary culture, to fabricate millimeter scale 3D tissues with homogeneous cell and ECM distribution.[20,21] To overcome the drawback of collagen hydrogels that often are stabilized using cytotoxic cross-linkers,[22] our group fabricated the novel material based on collagen microfibers (CMFs) which shows a good dispersibility in aqueous media. Moreover, fabricated CMFs are small enough to mix with cells homogeneously through simple pipetting. This feature solves the problem of heterogeneous cell distribution, typical of conventional seeding onto bulky collagen scaffolds.[23] To validate this strategy for cartilage tissues construction, type II collagen microfibers (CMF II) were selected and added to the identical number of the chondrogenic cells ATDC5. A series of histological assessments and quantitative phenotypic evaluations were conducted to unravel the interplay between the intercellular distance and the chondrogenic differentiation. Even though cell density is a crucial factor in ECM production, as shown for instance encapsulating different amounts of chondrocytes in collagen gels,[24] to date technologies that allow to both introduce ECM content and related mechanical signals on cells, while accurately tuning the cell−cell distance in 3D, are lacking. Addressing these challenges, to the best of our knowledge, this is the first report that investigates the impact on chondrocyte differentiation of CMF II amount and their function as intercellular spacers with microscale resolution as well as mechanical reinforcement element for engineered cartilage tissue. In this study, we also uncovered a possible mechanism of CMF determining chondrocytes phenotype via modulating N-cadherin expression. These findings will offer ways to construct functional zonal cartilage tissues.

2. MATERIALS AND METHODS

2.1. Materials. Medium A comprised Dulbecco's Modified Eagle Medium/Nutrient Mixture F-12 modified with GlutaMAX-supplement (DMEM/F12+GlutaMAX) (Gibco, Thermo Fisher Scientific, MA, U.S.A.), 5% fetal bovine serum (Gibco, Thermo Fisher Scientific, MA, U.S.A.), 1% antibiotic-antimycotic mixed solution (Nacalai Tesque, Kyoto, Japan), and 1% insulin-transferrin sodium selenite (ITS) liquid medium supplement (×100) purchased from Sigma-Aldrich (MO, U.S.A.). Medium B was based on medium A but with more supplements, 10 ng mL^{-1} Recombinant Human TGF-β1 (PeproTech, NJ, U.S.A.), 100 nmol L^{-1} Dexamethasone (Sigma-Aldrich, MO, Japan), and 0.2 mmol L^{-1} L-ascorbic acid-2-phosphate sesquimagnesium salt hydrate (Sigma-Aldrich, MO, Japan). The 24-well cell culture insert with 0.4 μm pore size was purchased from Corning (NY, U.S.A.), 6- and 24-well cell culture plates were purchased from Iwaki (Tokyo, Japan). For tissue fixation, 4% paraformaldehyde phosphate buffer solution (Nacalai Tesque, Kyoto, Japan) was selected. The ATDC5 cell line kindly donated by Prof. Itaka was used in cartilage tissue construction. Moreover, type II collagen derived from chicken was supplied by NH Foods Company (Osaka, Japan).

2.2. Fabrication of CMF II. CMF II were used as the basic scaffold to engineer the cartilage tissues. To harvest tailored CMF II (Figure S1 of the Supporting Information, SI), first, type II collagen was thermally cross-linked at 200 °C for 6 h to enhance the water stability in a vacuum sample drying oven (HD-15H, Ishii Laboratory Works, Osaka, Japan). Afterward, 50 mg cross-linked type II collagen was dissolved in 5 mL Milli-Q to acquire 1 wt % type II collagen solution. Then, it was treated by 6 min homogenization using a 10 mm diameter and 115 mm length homogenizer (VH-10, AS ONE, Osaka, Japan) followed by 29.2 min sonification (20 s sonication, 15 s cooling cycles) at 50 W electrical power using an ultrasonic processor (VC 50−1, Sonics & Materials, CT, U.S.A.). Subsequently, the collagen solution was filtrated by a 42 μm nylon mesh (PA-42u, AS ONE, Osaka, Japan). Finally, the collagen solution was lyophilized for 2 or 3 days.

2.3. Construction of 3D Differentiated Cartilage Tissues. To construct the 3D cartilage tissue with distinct intercellular distance, first, the CMF II was resuspended into medium A or B, respectively. Furthermore, the CMF II solution with the desired CMF II amount (0.9, 1.8, 4.5 mg) was mixed with 3×10^5ATDC5 cell homogeneously and seeded in 24-well cell culture inserts and centrifuged for 15 min at 1100*g*, successively. The control group II has undergone the same process but with removing the CMF II addition. Finally, inserts were assembled into 6-well plates filled with 11 mL medium that

https://dx.doi.org/10.1021/acsbiomaterials.0c00427
ACS Biomater. Sci. Eng. 2020, 6, 5711−5719

overflowed the top of the insets. The 3D cartilage tissue was incubated in 5% CO_2 at 37 °C for 1, 2, or 4 weeks differentiation, and its medium was refreshed every 3 or 4 days. For downstream histology analysis, the harvested cartilage tissues were fixed by 4% paraformaldehyde.

2.4. Histological and Immunohistochemical Stains. The fixed 3D cartilage tissues were submitted to the Applied Medical Research Company for paraffin embedding, section mounting, and histological staining procedures, including hematoxylin and eosin (HE) stain, toluidine blue stain, safranin O fast green stain, Col II, and Von Kossa stain. The stained cartilage tissue sections were observed by FL Evos Auto microscopy (Thermo Fisher Scientific, MA, U.S.A.) to get the brightfield images. In the case of safranin O fast green stain of native rat articular cartilage tissues given by Applied Medical Research Company was used for control comparisons. The superficial, middle, and deep zones were roughly distinguished by the percentage of the depth in full-thickness cartilage tissues and also chondrocytes morphology characteristics in distinct zones.[4]

2.5. Confirmation of Intercellular Distance Regulation. Toluidine blue staining brightfield images of constructed 3D cartilage tissues were analyzed by ImageJ. In the full-view of the image, the center cell instead of the one located in the surface of the tissues was chosen to measure the intercellular distances between them and four neighboring cells. Nuclei stained in blue were regarded as the starting and ending point of the intercellular distance measurement. To increase the reliability of the data, three more center cells were included, and the same process as mentioned before was undertaken. The distances were given by the ImageJ software. In each zone of natural rat articular cartilage tissues, 20 cells and their closest cells were measured to obtain the intercellular distance.

2.6. Glycosaminoglycan (GAG) Deposition Quantification. The whole experiment was guided by BlyscanSulfated Glycosaminoglycan Assay (Biocolor Life Science Assays, Antrim, U.K.). Briefly, the constructed cartilage tissues were digested by 145 μL papain extraction reagent for 18 h at 65 °C. After centrifugation, the supernatants containing GAG were adjusted to 100 μL with Milli-Q and bound to 1 mL Blyscan dye reagent. Finally, the GAG−dye complex was dissociated and further observed at 656 nm by a multimode reader (BioTek, Tokyo, Japan). The GAG value was calculated by a calibration curve related to the absorption intensity. Finally, the GAG secretion of each cell was acquired through understanding the relationship of cell proliferation and CMF II amounts (Figure S2).

2.7. Gene Expression Analyzed by RT-qPCR. The analyses of marker gene expression level were accessed by real-time quantitative polymerase chain reaction. To collect and purify the RNA, the 2D and 3D samples were treated by PureLink RNA Mini Kit (Invitrogen, Thermo Fisher Scientific, CA, U.S.A.) and Purelink DNase Set (Invitrogen, Thermo Fisher Scientific, CA, U.S.A.) for further removal of DNA contaminants. All RNA extraction procedures were strictly performed according to the instructions of the relevant protocol. Moreover, the RNA value was quantified using a Nanodrop 1000 apparatus (Thermo Fisher Scientific, MA, U.S.A.). The equivalent amount of RNA for each differentiation time was subsequently converted into cDNA by iScript cDNA Synthesis Kit (BioRAD, CA, U.S.A.). TaqMan Fast Advanced Master Mix (Applied Biosystems, Thermo Fisher Scientific, CA, U.S.A.) was used to initiate and amplify the cDNA. Additionally, TaqMan Gene Expression Assays (Applied Biosystems, Thermo Fisher Scientific, CA, U.S.A. Col2ac1: Mm01309565_m1; Sox9: Mm00448840_m1; Mmp13: Mm00439491_m1; Acan: Mm00545794_m1; Col10a1: Mm00487041_m1; Gapdh: Mm99999915_g1) were used to detect the specific fluorescence emission of target gene amplification. 44.4 ng and 64.2 ng cDNA template of 2 weeks and 4 weeks differentiation, respectively, were mixed with PCR reaction mix, and then added into a 48-well standard plate at a total volume of 20 μL.

The cDNA synthesis and RT-qPCR reaction were performed by StepOnePlus Real-Time PCR System (Thermo Fisher Scientific, MA, U.S.A.) under the guidance of the recommended heating program in the manual. 40 cycles of the denaturing and annealing processes were conducted for DNA amplification. The relative quantification of gene expressions was analyzed by the relative standard curve method. GAPDH was used as the endogenous control. 2D calibrator samples were obtained after 10^5ATDC5 cells were differentiated in a 24-well cell culture plate for 2 or 4 weeks. The fold-difference was estimated by the quotient of 3D cartilage tissues divided by 2D samples at identical differentiation times.

2.8. Mechanical Elastic Modulus Measurements. The 3D cartilage tissues were gently removed from the surface medium and harvested without the fixation treatment after 2 weeks differentiation in medium A. For native equine cartilage tissue, it was a gift from Utrecht university. Compression experiments were carried out to explore the mechanical behaviors under a 1 N loading cell by a 5 mm spherical indenter using an EZ-TEST instrument (Shimadzu, Kyoto, Japan) at a 1 mm min^{-1} loading speed. To eliminate any interference during the indention, only the stable range of 10 mN - 20 mN stress in the stress−strain curve was considered and further fitted into a linear slope. The elastic Young's modulus was automatically calculated by the instrument's own software.

2.9. Immunofluorescence Imaging. Constructed 3D cartilage tissues were fixed in 4% paraformaldehyde for 15 min at room temperature. Afterward, fix tissues went through the standard process of dehydration and G-NOX clearing (GenoStaff, Tokyo, Japan) through CT-Pro20 Cell & Tissue Processer (GenoStaff, Tokyo, Japan). Then, they were imbedded into paraffin and cut into 10 μm sections by microtome (Leica). The obtained paraffin sections were deparaffinized followed by heat mediated antigen retrieval. 10% normal goat serum (Wako, Osaka, Japan) in phosphate buffered saline (PBS) was used to block nonspecific binding. The primary antibody rabbit polyclonal anti human N-cadherin antibody (ab18203, Abcam, Cambridge, U.K.) at 1/200 dilution in 1% normal bovine serum albumin was used to bind the cadherin in the cell membrane because this antibody has cross-reactivity to mouse. After overnight incubation at 4 °C, the tissue slices were incubated with Alexa Fluor 488 conjugated goat anti rabbit IgG secondary antibody (AB-143165, Thermo Fisher Scientific, MA, U.S.A.) and 4′,6-diamidino-2-phenylindole (DAPI) (Thermo Fisher Scientific, MA, U.S.A.) for nuclei staining for 90 min incubation at room temperature. To eliminate the background noise from nonspecific binding or Fc receptor binding, a negative control rabbit IgG isotype (Thermo Fisher, MA, U.S.A.) was applied. Finally, the fabricated slices were rinsed in PBS and mounted by Fluoromount-G (Thermo Fisher, MA, U.S.A.) for fluorescence imaging through FV3000 confocal laser scanning microscopy (Olympus, Tokyo, Japan). The ratio of fluorescence signaling area was collected and quantified by ImageJ software. *N*-Cadherin positive staining area is acquired from separated channel of Alexa Flour 488.

2.10. Effect of Differentiation Time and CMF II Amount on Cell Proliferation. The DNA isolation of 2 or 4 weeks differentiated 3D cartilage tissue was conducted using a DNeasy Blood & Tissue Kit (QIAGEN, Hilden, Germany). Briefly, the cartilage tissues lysates were collected by proteinase K treatment and lysis buffer. After several purification processes, the DNA extract amount was measured by a Nanodrop 1000. The cell number was acquired after comparing the standard curve of cell number versus DNA amount. The standard curve was accessed by DNA amount quantification of 2D control samples with a known cell number.

2.11. Statistical Analysis. The data presented in this study were obtained from duplicate or three independent experiments. The results are expressed as means ± SD. The error bar represents the standard deviation. To test for significant differences, Student's *t*-tests were used to compare the differences of two groups. Values <0.05 were considered to be statistically significant. These are indicated in the graphs as $*p < 0.05$, $**p < 0.01$.

3. RESULTS AND DISCUSSION

3.1. Construction of 3D Cartilage Tissues with Tunable Intercellular Distances. First, the ATDC5 were mixed with various amounts of CMF II to construct the cartilage tissues with diverse intercellular distances. After

https://dx.doi.org/10.1021/acsbiomaterials.0c00427
ACS Biomater. Sci. Eng. 2020, 6, 5711−5719

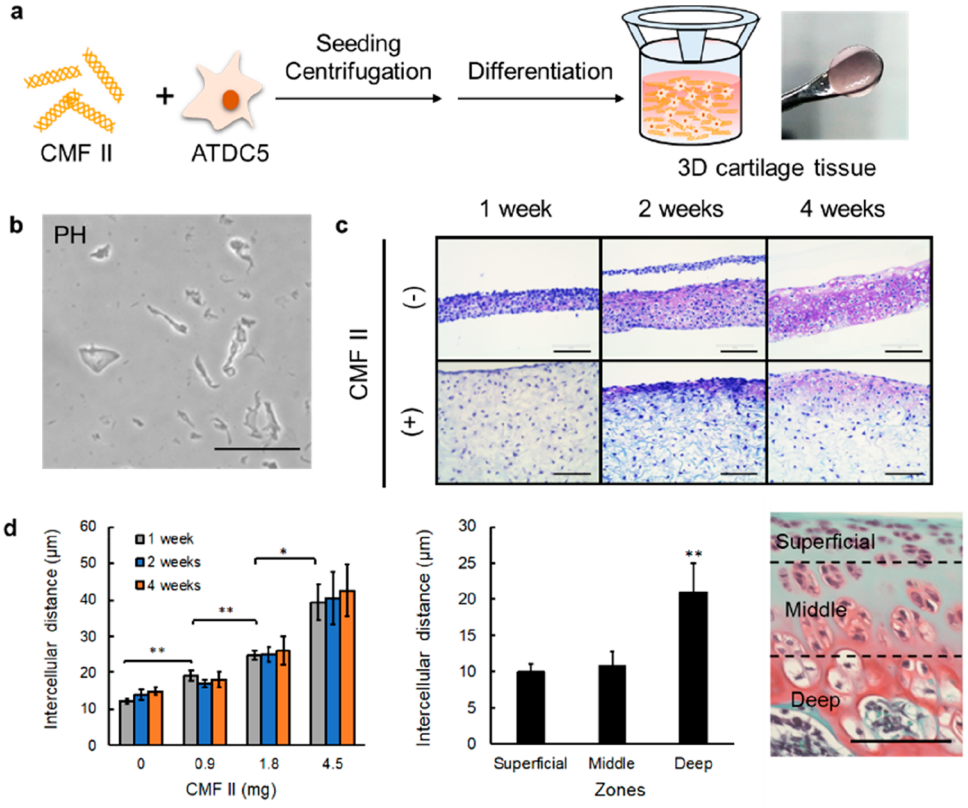

Figure 2. Fabrication of 3D cartilage tissues with different CMF II amounts. (a) Scheme for construction of 3D cartilage tissue via sedimentary culture. The right digital image shows a harvested cartilage tissue pellet. (b) Phase contrast (PH) image of fabricated representative CMF II. (c) Toluidine blue staining for visualization of intercellular distance change with or without CMF II after several weeks of differentiation. Nucleus were stained in blue color. (d) (left) Intercellular distance at diverse CMF II amounts after several weeks of differentiation. Four cells were chosen as the center cells randomly, the distances per center cell to four neighboring cells were measured to obtain the intercellular distance value (n = 16). (right) Intercellular distance of natural rat articular cartilage tissue in different zones (n = 10). Scale bar: 100 μm. *p < 0.05; **p < 0.01.

centrifugation and induction of differentiation in medium A based on DMEM/F12 with GlutaMAX-supplement, 5%FBS, 1% ITS liquid medium supplement, the resulting cartilage tissues were shaped in a transwell (Figure 2a). The fabricated collagen fiber material was characterized as being 52 ± 18 μm in length and having 12 ± 8 μm diameter fibers with high dispersibility after sequential physical processing (Figures 2b and S1). When mixing with cells, the microscale fibers enabled an even cell distribution, forming a homogeneous interconnection, which is a great advantage over traditional porous collagen scaffolds (Figures 3a and S3). Most importantly, the intercellular distance was elevated gradually by increasing the amount of CMF II in the cartilage tissues independent of differentiation time (Figure 2c,d). Additionally, modulating the amount of CMF, it was possible to achieve intercellular distances in a range comparable to that of human articular cartilage tissues, it is expected to mimic the in vivo situation and cellular distribution.

3.2. Assessment of Cell Behavior in Engineered Cartilage Tissues with Various Intercellular Distances. According to HE staining images, CMF II containing groups indicated a dense and thin cell layer in the surfaces while leaving sparse cell thick tissues in the center. The same phenomenon was not detected in the control groups due to the absence of CMF II (Figure 3a,e,i,m,q,u). There was not enough space in the control groups to migrate and proliferate quickly to make a gradient structure. We hypothesized that the favorable interfacial environment such as sufficient oxygen supply and relatively fresh nutrients facilitated the cell expansion. Toluidine blue staining indicating that GAG production was upregulated in the control group, in other words, in the group with the shortest intercellular distance (Figure 3b,f,j,n,r,v). In the CMF II containing groups, the GAG staining was much stronger on the construct surface area compared to the negatively stained inside. It could be rationalized that concentrated CMF II, favoring cell−ECM interaction over cell−cell interconnections, hampered cell aggregation during the early stage of chondrogenesis leading to decreased cartilaginous matrix production. This finding is quite interesting because the scaffold-free cartilage tissue (control) shows intensive matrix staining in the central area on account of the higher aggregation within the construct. Additionally, a slight proteoglycan secretion was only discovered in the 4 week differentiated control groups in the Safranin O fast green staining indicated by the black arrow in Figure 3o, but not in the groups containing CMFII in Figure 3c,g,k,s,w. The differentiation medium of transforming growth factor-β1 (TGF-β1), a powerful and well-established chondrogenic factor (indicated as medium B in this study), showed a higher secretion of chondrocyte-specific ECM (Figure S4). The abundance of type II collagen found in all groups suggested establishment of cartilaginous matrix-rich tissues although it was not possible to distinguish the endogenous type II collagen and exogenous CMF II because of the cross-reaction of the antibody (Figures 3d,h,l,p,t,x and S5). The engineered cartilage tissues showed negative to Von Kossa staining, suggesting

https://dx.doi.org/10.1021/acsbiomaterials.0c00427
ACS Biomater. Sci. Eng. 2020, 6, 5711−5719

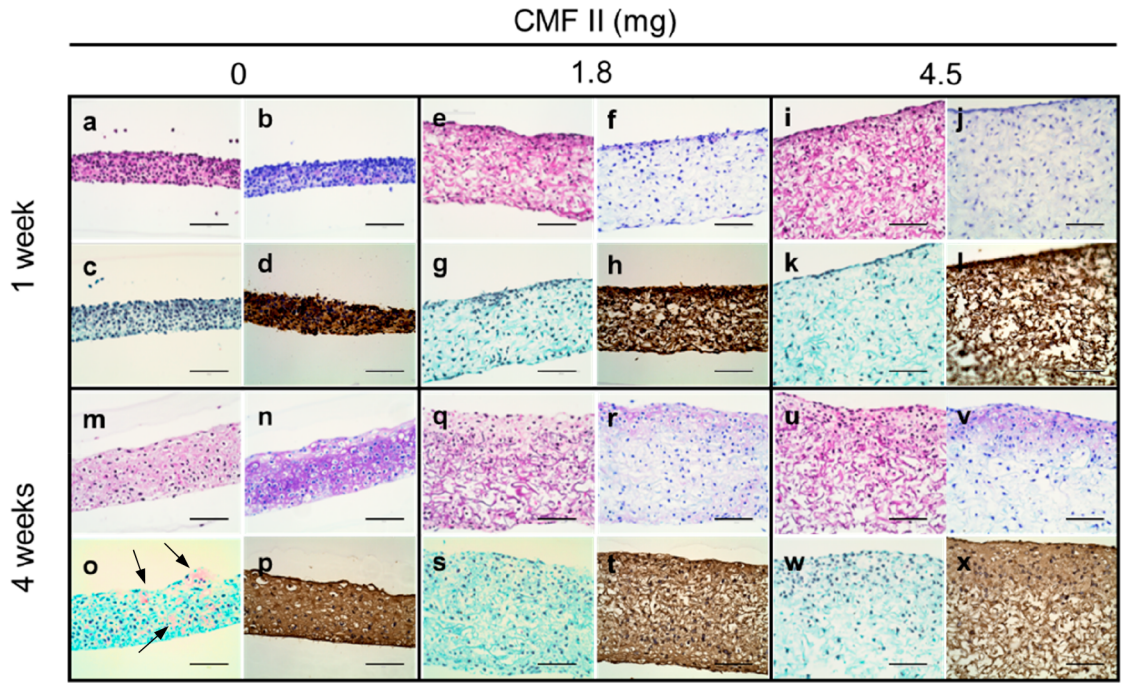

Figure 3. Histological evaluation of constructed cartilage tissues with various differentiation times and CMF II amounts. (a), (e), (i), (m), (q), and (u) are assigned to Hematoxylin-Eosin stain, purple and pink indicate chondrocyte nucleus and extracellular matrix, respectively. (b), (f), (j), (n), (r), and (v) are cartilage tissue sections stained by toluidine blue. Purple represents the secreted glycosaminoglycan (GAG). Safranin O fast green stain is presented in (c), (g), (l), (o), (s), and (w). The cartilaginous proteoglycan (red) was observed in the 4 weeks differentiated 0 mg CMF II group o suggested by black arrows. (d), (h), (l), (p), (t), and (x) are assigned to type II collagen (Col II) immunohistochemistry stains. Cartilage tissues colored in brown suggest the existence of both endogenous and exogenous type II collagen. Scale bar: 100 μm.

ossification did not happen after 4 weeks differentiation (Figure S6). Quantifications of GAG deposition were performed to further evaluate the influence of intercellular distance on characteristic ECM production (Figure 4). The

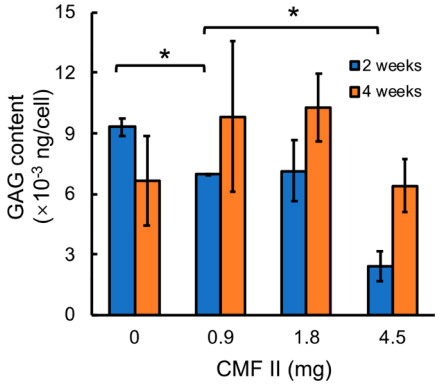

Figure 4. GAG secretion determined by CMF II and differentiation time. GAG was stained by 1,9-dimethylmethylene blue and its content was subjected to an absorbance intensity of 656 nm conducted by Blyscan Sulfated Glycosaminoglycan assay. GAG values are expressed as the means ± SD n = 2; *p < 0.05.

GAG secretion levels were in accordance with the observations from toluidine blue staining (Figure S3) in 2 weeks differentiation groups. The GAG secretion was suppressed in the higher CMF II content group associated with longer intercellular distance. Although GAG secretion of control groups after 4 weeks differentiation was lower than that of 2 weeks of differentiation groups, CMF II containing groups after 4 weeks of differentiation indicated higher GAG secretion than those of 2 weeks of differentiations. Chondrocytes increasing at least 10 times after differentiation culture indicates a great potential of proliferation (Figure S2).

3.3. Regulation of Marker Gene Expression through Tuning Intercellular Distances. To understand the relationship between chondrocyte differentiation and cell−cell distance, real time RT-PCR analyses were performed for 2 and 4 weeks using 2D monolayer chondrocytes with same differentiation condition as a calibrator sample. In Figure 5, it presents an elevation of chondrogenic maker genes expression including ACAN, COL2A1in the control groups after 4 weeks of differentiation together with hypertrophic markers MMP13 and COL10A1. The gene expressions of the CMF II samples after 4 weeks were also higher than those of 2 weeks, but lower than the control samples. The ACAN, COL2A1, MMP13 gene expression levels of control groups and 1.8 mg CMF II have relatively big error bars among the three samples (n = 3) after 4 weeks of differentiation. However, the tendency might be consistent with our anticipation that CMF II has an inhibitory effect on chondrogenesis. Because, MMP13 acting as a matric degeneration enzyme could be a clue to understand the apoptosis caused by osteoarthritis.[25] It may come into a conclusion that introducing CMF II decelerates the progress of osteoarthritis that inhibit apoptosis. SOX9, a transcription factor is regarded as a key regulator to dictate the chondrocyte differentiation and above chondrocyte-specific ECM gene expressions.[26,27] It was surprising that no obvious difference of SOX9 expression within all tested groups even higher ECM gene expressions, may suggest keeping the chondrocyte phenotype. Furthermore, the steady SOX9 gene expression is coincident with the observation of almost comparable cell growth (Figure S2).

https://dx.doi.org/10.1021/acsbiomaterials.0c00427
ACS Biomater. Sci. Eng. 2020, 6, 5711−5719

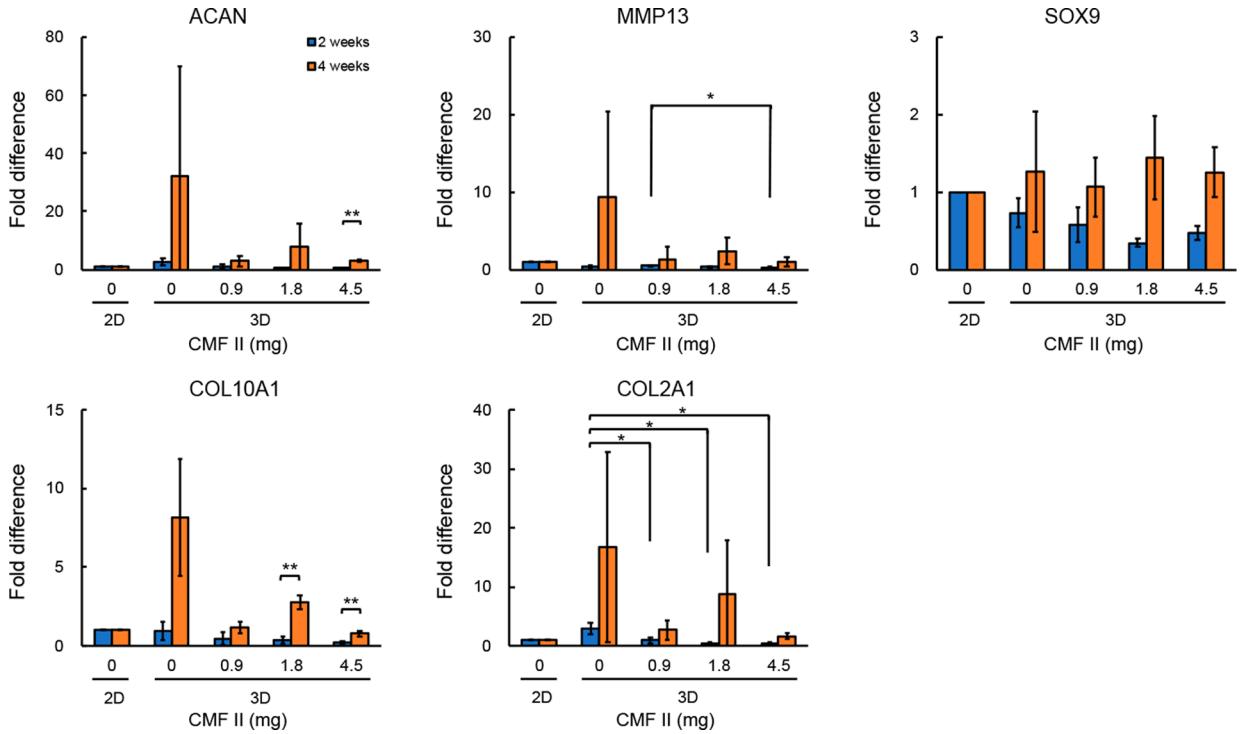

Figure 5. Real-time RT-PCR analyses of marker gene expression of differentiated 3D cartilage tissues after two or 4 weeks of differentiation. RNA expression levels were normalized to the level of GAPDH expression. Each RNA expression was evaluated by 3 parallel cartilage tissue samples under the same conditions (n = 3). Fold difference was estimated by the relative expression comparing constructed 3D cartilage tissues and 2D monolayer chondrocytes with same differentiation conditions for calibration. The gene expression of 2D monolayer chondrocytes is equal to one. Each sample was duplicated to eliminate technical mistakes. *p < 0.05; **p < 0.01.

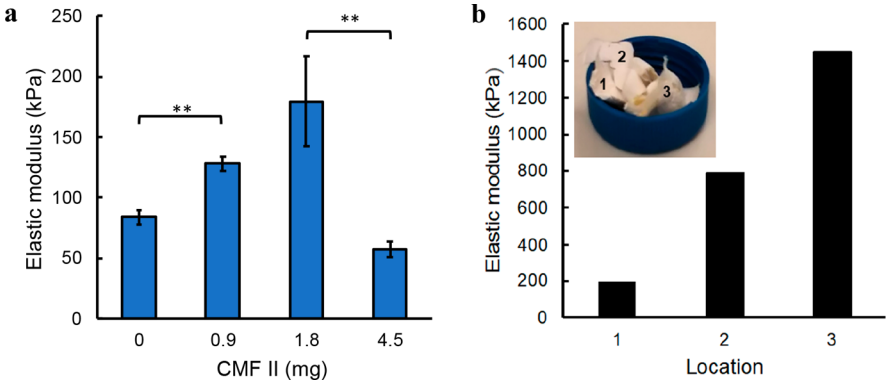

Figure 6. Mechanical properties of (a) CMF II-strengthened cartilage tissue and (b) native equine cartilage tissues. The constructed cartilage tissues were collected after 2 weeks differentiation and compressed by a 5 mm diameter spherical indenter at room temperature using an EZ-TEST instrument (n = 3; **p < 0.01). The elastic modulus was measured in three different pieces of one equine articular cartilage tissue.

3.4. Enhancement of the Mechanical Strength of Cartilage Tissues by Using CMF II. To understand the crosstalk between mechanical properties and CMF II amount, elastic modulus of each sample was evaluated after 2 weeks differentiation by compression tests. The elastic modulus increased proportionately to the CMF II amount when CMF II amount is below 1.8 mg (Figure 6a). Once an excess amount (4.5 mg) of CMF II was added into the cartilage tissues, a sharp decline of mechanical strength was observed. We assumed that with the help of cell−cell interaction through adjacent conjugation of N-cadherin and cell−matrix interaction through the integrin connection, cartilage tissues were strengthened to withstand the external force.[28,29] It is expected that overloaded 4.5 mg CMF II groups rendered the excessive CMF II accumulated in the interior of the cartilage tissues that reduced the cell concentration and further blocked the cell−cell and cell−matrix interactions. However, the elastic modulus of the pieces of native equine cartilage tissues was much higher than the constructed cartilage tissues, only the stiffest 1.8 mg CMF II group was equivalent to the lowest level of the native tissues (Figure 6b).

3.5. Discoveries of the Interplay between Intercellular Distance and N-Cadherin Expression. Intercellular communication is believed to be a key factor in chondrogenesis progress especially in the condensation phase. Adhesion molecule N-cadherin was reported to play a great role in cell−cell contacts thus help subsequent chondrogenesis.[30,31] To rationalize the findings that differentiation is

https://dx.doi.org/10.1021/acsbiomaterials.0c00427
ACS Biomater. Sci. Eng. 2020, 6, 5711−5719

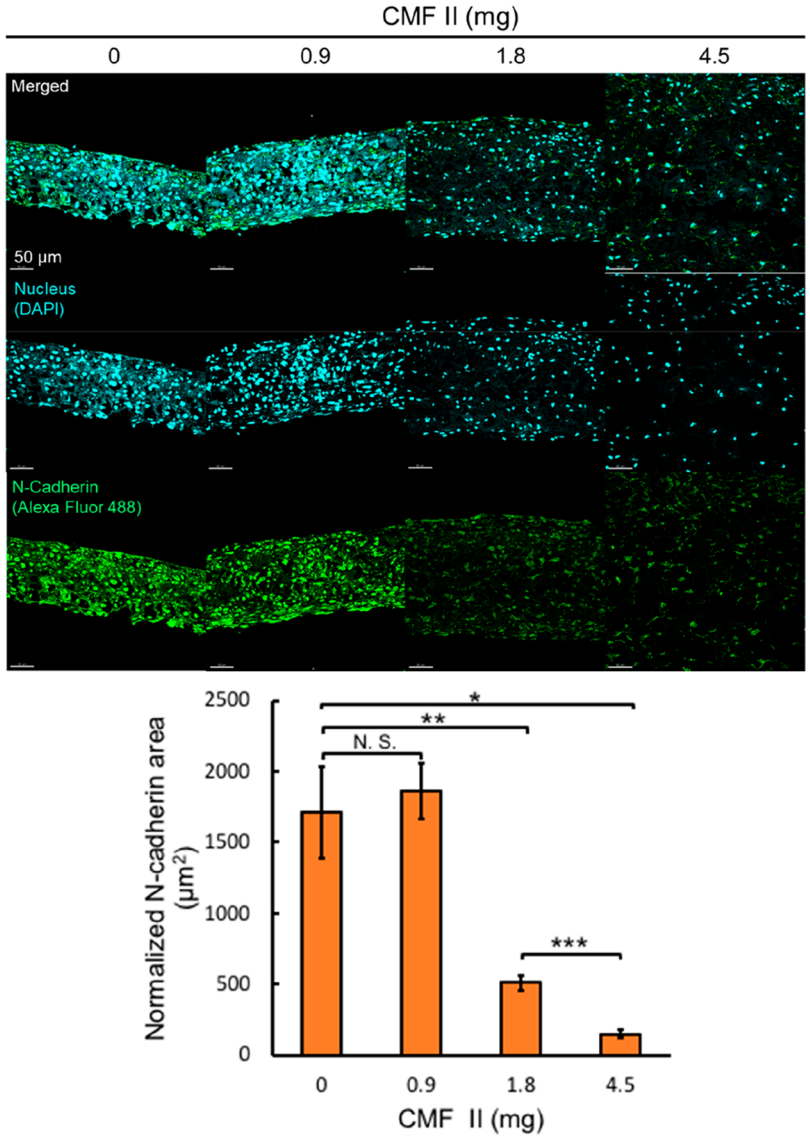

Figure 7. N-Cadherin positive staining area was governed by chondrocyte density. The fluorescence images presented 4 weeks differentiated cartilage tissues. N-Cadherin is indicated in green by Alexa Fluor 488 and nucleus is indicated in blue by DAPI. The positive staining area of N-cadherin is evaluated by the N-cadherin fluorescence area normalized by intercellular distances. N.S., no significance; $n = 3$; *$p < 0.05$; **$p < 0.01$; ***$p < 0.001$.

determined by intercellular distance, we next stained the N-cadherin in different test groups (Figure 5). N-Cadherin highlighted in green fluorescence was well visible in control groups, however the signals declined with increasing the amounts of CMF II from 0.9 to 4.5 mg (Figures 7a and S7). This trend was also confirmed by measuring N-cadherin positive area in the sections (Figure 7b), in which the sections of CMF II 1.8 and 4.5 mg had significantly lower the positive area than those of 0 and 0.9 mg, although there is no significant difference between 0 mg CMF II and 0.9 mg CMF II containing groups. These results are consistent to the expression profiles of chondrogenesis makers (Figure 5), further highlighting the effects of this system on regulating the chondrogenesis by changing intercellular distances.

4. CONCLUSIONS

Herein, we presented a novel technology to modulate chondrocyte differentiation by simply adjusting the intercellular distance using CMF II. The engineered cartilage tissue containing CMF II showed a greater ability to diminish the development of chondrogenesis while keeping the ability of the embedded cells to express chondrogenic markers. In contrast, the control and 0.9 mg groups displayed a higher marker gene expression including chondrogenesis genes (ACAN, COL2A1) and hypertrophic genes (MMP13, COL10A1). Moreover, it exhibited a decreasing trend of GAG production when increasing intercellular distance after 2 weeks differentiation which further confirmed its superior capacity of differentiation control in a protein level. As a result of the proof of concept, the intercellular distance change facilitates the control of chondrocyte differentiation by using CMF II through possibly regulating the *N*-cadherin expression (Figure 8). This system may be applied for modulating the differentiation of other cell sources, and further investigation with different cell type should be considered in future steps. We expect this cartilage tissue construction strategy will offer new opportunities for performing drug assays as an OA model or for use as therapeutic implants in the near future.

https://dx.doi.org/10.1021/acsbiomaterials.0c00427
ACS Biomater. Sci. Eng. 2020, 6, 5711−5719

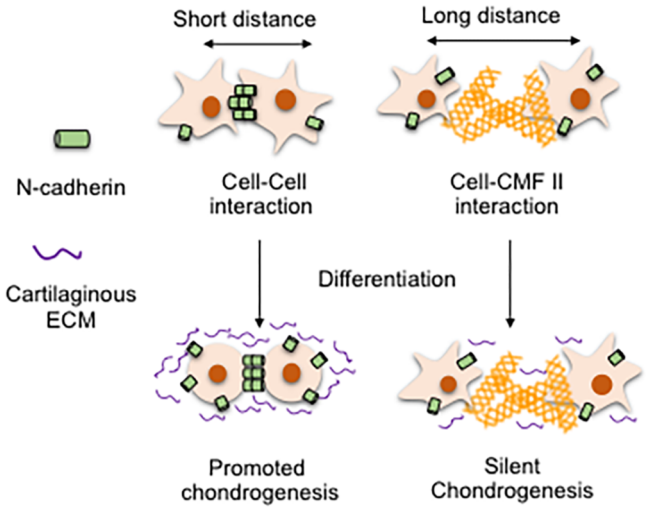

Figure 8. Differentiation regulation using CMF II. Adjustable distances governed by CMF II amount determined major interaction during differentiation that determined the consequent chondrocyte phenotype.

■ ASSOCIATED CONTENT

Supporting Information

The Supporting Information is available free of charge at https://pubs.acs.org/doi/10.1021/acsbiomaterials.0c00427.

Figure S1, Workflows of CMF II; Figure S2, cell growth of constructed cartilage tissues; Figure S3, histologic evaluation of constructed cartilage tissues after 2 weeks differentiation in medium A; Figure S4, histologic evaluation of medium B differentiated constructed cartilage tissues; Figure S5, Col II immunohistochemistry staining; Figure S6, Von Kossa staining; and Figure S7, N-cadherin immunofluorescence staining (PDF)

■ AUTHOR INFORMATION

Corresponding Author

Michiya Matsusaki − *Department of Applied Chemistry, Graduate School of Engineering and Joint Research Laboratory (TOPPAN) for Advanced Cell Regulatory Chemistry, Graduate School of Engineering, Osaka University, Osaka 565-0871, Japan;* orcid.org/0000-0003-4294-9313; Phone: +81-6-6879-7356; Email: m-matsus@chem.eng.osaka-u.ac.jp; Fax: +81-6-6879-7359

Authors

Jinyu Li − *Department of Applied Chemistry, Graduate School of Engineering, Osaka University, Osaka 565-0871, Japan*

Naoko Sasaki − *Joint Research Laboratory (TOPPAN) for Advanced Cell Regulatory Chemistry, Graduate School of Engineering, Osaka University, Osaka 565-0871, Japan*

Keiji Itaka − *Department of Biofunction Research, Institute of Biomaterials and Bioengineering, Tokyo Medical and Dental University (TMDU), Tokyo 101-0062, Japan*

Margo Terpstra − *Department of Orthopaedics, University Medical Center Utrecht, Utrecht University, Utrecht 3584CX, The Netherlands*

Riccardo Levato − *Department of Orthopaedics, University Medical Center Utrecht and Department of Clinical Sciences, Faculty of Veterinary Medicine, Utrecht University, Utrecht 3584CX, The Netherlands;* orcid.org/0000-0002-3795-3804

Complete contact information is available at: https://pubs.acs.org/10.1021/acsbiomaterials.0c00427

Author Contributions

The paper was written through contributions of all the authors. All the authors have given approval to the final version of the paper.

Notes

The authors declare no competing financial interest.

■ ACKNOWLEDGMENTS

This study was partly sponsored by Osaka University and partly financially supported by Grant-in-Aid for Scientific Research (B) (17H02099 and 19H03776). R.L. acknowledges the funding from the ReumaNederland (LLP-12 and LLP22), and from Hofvijverkring Fellowship programme. The authors are grateful for the donation of collagen from the NH Foods Company.

■ ABBREVIATIONS

CMF II, type II collagen microfibers; CMFs, collagen microfibers; ACI, autologous cartilage implantation; MSCs, mesenchymal stem cells; ACPCs, articular cartilage-resident chondroprogenitor cells; ITS, insulin-transferrin sodium selenite; HE, hematoxylin and eosin; GAG, glycosaminoglycan; PBS, phosphate buffered saline; DAPI, 4′,6-diamidino-2-phenylindole; TGF-β1, transforming growth factor-β1

■ REFERENCES

(1) GBD 2015 Disease and Injury Incidence and Prevalence Collaborators. Global, Regional, and National Incidence, Prevalence, and Years Lived with Disability for 310 Diseases and Injuries, 1990−2015: A Systematic Analysis for the Global Burden of Disease Study 2015. *Lancet* **2016**, *388* (10053), 1545−1602.

(2) Baugé, C.; Boumédiene, K. Use of Adult Stem Cells for Cartilage Tissue Engineering: Current Status and Future Developments. *Stem Cells Int.* **2015**, *2015*, 1−14.

(3) Goldring, M. B. Chondrogenesis, Chondrocyte Differentiation, and Articular Cartilage Metabolism in Health and Osteoarthritis. *Ther. Adv. Musculoskeletal Dis.* **2012**, *4* (4), 269−285.

(4) Sophia Fox, A. J.; Bedi, A.; Rodeo, S. A. The Basic Science of Articular Cartilage. *Sports Health* **2009**, *1* (6), 461−468.

(5) Antons, J.; Marascio, M. G. M.; Nohava, J.; Martin, R.; Applegate, L. A.; Bourban, P. E.; Pioletti, D. P. Zone-Dependent Mechanical Properties of Human Articular Cartilage Obtained by Indentation Measurements. *J. Mater. Sci.: Mater. Med.* **2018**, *29* (5), 57.

(6) Yamashita, A.; Morioka, M.; Yahara, Y.; Okada, M.; Kobayashi, T.; Kuriyama, S.; Matsuda, S.; Tsumaki, N. Generation of Scaffoldless Hyaline Cartilaginous Tissue from Human IPSCs. *Stem Cell Rep.* **2015**, *4* (3), 404−418.

(7) Stuart, M. P.; Matsui, R. A. M.; Santos, M. F. S.; Côrtes, I.; Azevedo, M. S.; Silva, K. R.; Beatrici, A.; Leite, P. E. C.; Falagan-Lotsch, P.; Granjeiro, J. M.; Mironov, V.; Baptista, L. S. Successful Low-Cost Scaffold-Free Cartilage Tissue Engineering Using Human Cartilage Progenitor Cell Spheroids Formed by Micromolded Nonadhesive Hydrogel. *Stem Cells Int.* **2017**, *2017*, 1−11.

(8) Chen, S.; Zhang, Q.; Nakamoto, T.; Kawazoe, N.; Chen, G. Gelatin Scaffolds with Controlled Pore Structure and Mechanical Property for Cartilage Tissue Engineering. *Tissue Eng., Part C* **2016**, *22* (3), 189−198.

(9) Wang, C.-C.; Yang, K.-C.; Lin, K.-H.; Liu, Y.-L.; Liu, H.-C.; Lin, F.-H. Cartilage Regeneration in SCID Mice Using a Highly Organized Three-Dimensional Alginate Scaffold. *Biomaterials* **2012**, *33* (1), 120−127.

(10) Foss, C.; Merzari, E.; Migliaresi, C.; Motta, A. Silk Fibroin/Hyaluronic Acid 3D Matrices for Cartilage Tissue Engineering. *Biomacromolecules* **2013**, *14* (1), 38−47.
(11) Yin, L.; Wu, Y.; Yang, Z.; Denslin, V.; Ren, X.; Tee, C. A.; Lai, Z.; Lim, C. T.; Han, J.; Lee, E. H. Characterization and Application of Size-Sorted Zonal Chondrocytes for Articular Cartilage Regeneration. *Biomaterials* **2018**, *165*, 66−78.
(12) Levato, R.; Webb, W. R.; Otto, I. A.; Mensinga, A.; Zhang, Y.; van Rijen, M.; van Weeren, R.; Khan, I. M.; Malda, J. The Bio in the Ink: Cartilage Regeneration with Bioprintable Hydrogels and Articular Cartilage-Derived Progenitor Cells. *Acta Biomater.* **2017**, *61*, 41−53.
(13) Zhu, D.; Tong, X.; Trinh, P.; Yang, F. Mimicking Cartilage Tissue Zonal Organization by Engineering Tissue-Scale Gradient Hydrogels as 3D Cell Niche. *Tissue Eng., Part A* **2018**, *24*, 157−167.
(14) Cohen, N. P.; Foster, R. J.; Mow, V. C. Composition and Dynamics of Articular Cartilage: Structure, Function, and Maintaining Healthy State. *J. Orthop Sports Phys. Ther* **1998**, *28* (4), 203−215.
(15) Lian, C.; Wang, X.; Qiu, X.; Wu, Z.; Gao, B.; Liu, L.; Liang, G.; Zhou, H.; Yang, X.; Peng, Y.; Liang, A.; Xu, C.; Huang, D.; Su, P. Collagen Type II Suppresses Articular Chondrocyte Hypertrophy and Osteoarthritis Progression by Promoting Integrin B1-SMAD1 Interaction. *Bone Res.* **2019**, *7* (1), 8.
(16) Cao, B.; Li, Z.; Peng, R.; Ding, J. Effects of Cell−Cell Contact and Oxygen Tension on Chondrogenic Differentiation of Stem Cells. *Biomaterials* **2015**, *64*, 21−32.
(17) Schrobback, K.; Klein, T. J.; Woodfield, T. B. F. The Importance of Connexin Hemichannels During Chondroprogenitor Cell Differentiation in Hydrogel Versus Microtissue Culture Models. *Tissue Eng., Part A* **2015**, *21* (11−12), 1785−1794.
(18) Cosgrove, B. D.; Mui, K. L.; Driscoll, T. P.; Caliari, S. R.; Mehta, K. D.; Assoian, R. K.; Burdick, J. A.; Mauck, R. L. N-Cadherin Adhesive Interactions Modulate Matrix Mechanosensing and Fate Commitment of Mesenchymal Stem Cells. *Nat. Mater.* **2016**, *15* (12), 1297−1306.
(19) Vega, S. L.; Kwon, M. Y.; Song, K. H.; Wang, C.; Mauck, R. L.; Han, L.; Burdick, J. A. Combinatorial Hydrogels with Biochemical Gradients for Screening 3D Cellular Microenvironments. *Nat. Commun.* **2018**, *9* (1), 614.
(20) Su, D.; Teoh, C. L.; Park, S.-J.; Kim, J.-J.; Samanta, A.; Bi, R.; Dinish, U. S.; Olivo, M.; Piantino, M.; Louis, F.; Matsusaki, M.; Kim, S. S.; Bae, M. A.; Chang, Y.-T. Seeing Elastin: A Near-Infrared Zwitterionic Fluorescent Probe for In Vivo Elastin Imaging. *Chem.* **2018**, *4* (5), 1128−1138.
(21) Louis, F.; Kitano, S.; Mano, J. F.; Matsusaki, M. 3D Collagen Microfibers Stimulate the Functionality of Preadipocytes and Maintain the Phenotype of Mature Adipocytes for Long Term Cultures. *Acta Biomater.* **2019**, *84*, 194−207.
(22) Yang, K.; Sun, J.; Wei, D.; Yuan, L.; Yang, J.; Guo, L.; Fan, H.; Zhang, X. Photo-Crosslinked Mono-Component Type II Collagen Hydrogel as a Matrix to Induce Chondrogenic Differentiation of Bone Marrow Mesenchymal Stem Cells. *J. Mater. Chem. B* **2017**, *5* (44), 8707−8718.
(23) Tamaddon, M.; Burrows, M.; Ferreira, S. A.; Dazzi, F.; Apperley, J. F.; Bradshaw, A.; Brand, D. D.; Czernuszka, J.; Gentleman, E. Monomeric, Porous Type II Collagen Scaffolds Promote Chondrogenic Differentiation of Human Bone Marrow Mesenchymal Stem Cells in Vitro. *Sci. Rep.* **2017**, *7* (1), 43519.
(24) Ren, X.; Wang, F.; Chen, C.; Gong, X.; Yin, L.; Yang, L. Engineering Zonal Cartilage through Bioprinting Collagen Type II Hydrogel Constructs with Biomimetic Chondrocyte Density Gradient. *BMC Musculoskeletal Disord.* **2016**, *17* (1) DOI: 10.1186/s12891-016-1130-8.
(25) Lotz, M.; Hashimoto, S.; Kühn, K. Mechanisms of chondrocyte apoptosis. *Osteoarthritis and cartilage* **1999**, *7* (4), 389−391.
(26) Bi, W.; Deng, J. M.; Zhang, Z.; Behringer, R. R.; de Crombrugghe, B. Sox9 Is Required for Cartilage Formation. *Nat. Genet.* **1999**, *22* (1), 85−89.
(27) Akiyama, H. The Transcription Factor Sox9 Has Essential Roles in Successive Steps of the Chondrocyte Differentiation Pathway and Is Required for Expression of Sox5 and Sox6. *Genes Dev.* **2002**, *16* (21), 2813−2828.
(28) Sivasankar, S. Tuning the Kinetics of Cadherin Adhesion. *J. Invest. Dermatol.* **2013**, *133* (10), 2318−2323.
(29) Kechagia, J. Z.; Ivaska, J.; Roca-Cusachs, P. Integrins as Biomechanical Sensors of the Microenvironment. *Nat. Rev. Mol. Cell Biol.* **2019**, *20* (8), 457−473.
(30) Delise, A. M.; Tuan, R. S. Analysis of N-Cadherin Function in Limb Mesenchymal Chondrogenesis in Vitro. *Dev. Dyn.* **2002**, *225* (2), 195−204.
(31) Conacci-Sorrell, M.; Simcha, I.; Ben-Yedidia, T.; Blechman, J.; Savagner, P.; Ben-Ze'ev, A. Autoregulation of E-Cadherin Expression by Cadherin−Cadherin Interactions. *J. Cell Biol.* **2003**, *163* (4), 847−857.

https://dx.doi.org/10.1021/acsbiomaterials.0c00427
ACS Biomater. Sci. Eng. 2020, 6, 5711−5719